stress during carcinogenesis, Mutat. Res. 387 (1997) 147–163.
[25] D. Sagher, B. Strauss, Insertion of nucleotides opposite apurinic/apyrimidinic sites in deoxyribonucleic acid during in vitro synthesis: uniqueness of adenine nucleotides, Biochemistry 22 (1983) 4518–4526.
[26] M.S. Greenblatt, W.P. Bennett, M. Hollstein, C.C. Harris, Mutations in the p53 tumor suppressor gene: clues to cancer etiology and molecular pathogenesis, Cancer Res. 54 (1994) 4855–4878.
[27] P. Hainaut, T. Hernandez, A. Robinson, P. Rodriguez-Tome, T. Flores, M. Hollstein, C.C. Harris, R. Montesano, IARC Database of p53 gene mutations in human tumors and cell lines: updated compilation, revised formats and new visualisation tools, Nucleic Acids Res. 26 (1998) 205–213.
[28] S. Shibutani, M. Takeshita, A.P. Grollman, Insertion of specific bases during DNA synthesis past the oxidation-damaged base 8-oxodG, Nature 349 (1991) 431–434.
[29] C.J. Burrows, J.G. Muller, O. Kornyushyna, W. Luo, V. Duarte, M.D. Leipold, S.S. David, Structure and potential mutagenicity of new hydantoin products from guanosine and 8-oxo-7,8-dihydroguanine oxidation by transition metals, Environ. Health Perspect. 110 (Suppl. 5) (2002) 713–717.
[30] P.D. Chastain II, J. Nakamura, J. Swenberg, D. Kaufman, Nonrandom AP site distribution in highly proliferative cells, FASEB J. 20 (2006) E2127–E2132.
[31] D.-S. Duan, W. Sadee, Guanine for DNA synthesis: a compulsory route through ribonucleotide reductase, Biochem. J. 255 (1988) 1045–1048.
[32] H. Hayakawa, A. Hofer, L. Thelander, S. Kitajima, Y. Cai, S. Oshiro, H. Yakushiji, Y. Nakabeppu, M. Kuwano, M. Sekiguchi, Metabolic fate of oxidized guanine ribonucleotides in mammalian cells, Biochemistry 38 (1999) 3610–3614.
[33] D.S. Chen, T. Herman, B. Demple, Two distinct human DNA diesterases that hydrolyze 3'-blocking deoxyribose fragments from oxidized DNA, Nucleic Acids Res. 19 (1991) 5907–5914.
[34] G.L. Dianov, K.M. Sleeth, Dianova II, S.L. Allinson, Repair of abasic sites in DNA, Mutat. Res. 531 (2003) 157–163.
[35] T. Sawa, M.H. Zaki, T. Okamoto, T. Akuta, Y. Tokutomi, S. Kim-Mitsuyama, H. Ihara, A. Kobayashi, M. Yamamoto, S. Fujii, H. Arimoto, T. Akaike, Protein S-guanylation by the biological signal 8-nitroguanosine 3',5'-cyclic monophosphate, Nat. Chem. Biol. 3 (2007) 727–735.
[36] H. Ohshima, H. Tazawa, B.S. Sylla, T. Sawa, Prevention of human cancer by modulation of chronic inflammatory processes, Mutat. Res. 591 (2005) 110–122.
[37] M.M. Chan, H.I. Huang, M.R. Fenton, D. Fong, In vivo inhibition of nitric oxide synthase gene expression by curcumin, a cancer preventive natural product with anti-inflammatory properties, Biochem. Pharmacol. 55 (1998) 1955–1962.
[38] A. Murakami, K. Matsumoto, K. Koshimizu, H. Ohigashi, Effects of selected food factors with chemopreventive properties on combined lipopolysaccharide- and interferon-gamma-induced IkappaB degradation in RAW264.7 macrophages, Cancer Lett. 195 (2003) 17–25.

Jpn. J. Infect. Dis., 61, 157-160, 2008

Short Communication

H5N1-Infected Cells in Lung with Diffuse Alveolar Damage in Exudative Phase from a Fatal Case in Vietnam

Nguyen Thanh Liem, Noriko Nakajima[1], Le Phuc Phat**, Yuko Sato[1], Hoang Ngoc Thach, Pham Viet Hung, Luong Thi San, Harutaka Katano[1], Toshio Kumasaka[1,2], Teruaki Oka[3], Shoji Kawachi[4], Takeji Matsushita[4], Tetsutaro Sata[1], Koichiro Kudo[4] and Kazuo Suzuki[1,5]*

The National Hospital of Pediatrics, Hanoi, Vietnam; [1]National Institute of Infectious Diseases, Tokyo 162-8640; [2]Juntendo University School of Medicine, Tokyo 113-8421; [3]Kanto Central Hospital, Tokyo 158-8531; [4]International Medical Center of Japan, Tokyo 162-8655; and [5]Chiba University Graduate School of Medicine, Chiba 260-8670, Japan

(Received October 23, 2007. Accepted February 4, 2008)

SUMMARY: Necropsied lung tissues of three fatal cases with avian influenza A virus (H5N1) infection in Vietnam were analyzed to detect H5N1 virus-infected cells. Formalin-fixed and paraffin-embedded lung tissue sections showed typical histological features of diffuse alveolar damage (DAD) in all cases. Immunohistochemistry for the influenza A virus nucleoprotein antigen revealed positive signals of bronchiolar and alveolar epithelial cells in only one patient, who exhibited DAD with an exudative phase and died on the 6th day after onset. However, no signal was detected in the other two cases of DAD with a proliferative phase. These patients died on day 16 and day 17 after onset, respectively. H5N1 virus antigens were detected predominantly in epithelial cells in terminal bronchioles and in alveoli, i.e., type I and type II alveolar pneumocytes, and in alveolar macrophages. The pathogenesis of exudative DAD caused by H5N1 infection is discussed.

Highly pathogenic avian influenza A H5N1 virus (H5N1) infection has been reported to cause severe respiratory disease. In 1997, H5N1 was first isolated in Hong Kong from tracheal aspirates of a 3-year-old boy with a fatal respiratory illness (1-3). In 2003, human disease associated with H5N1 re-emerged (4). Since then, the number of confirmed fatal human H5N1-infected cases has increased and now totals approximately 200 cases. These cases occurred, predominantly, in Vietnam, Thailand, and Indonesia (5-9). The histopathological data for H5N1 virus infection in humans were, however, limited (3,4,6,8,10-12), and the pathogenesis of the disease remains unclear. Examination of ex vivo infected lung tissues showed that influenza A virus nucleoprotein (InfA-NP) was detected in pneumocytes and in alveolar macrophages (13). Also the pattern of viral attachment in human respiratory tract sections showed that H5N1 attached to the apical cell membrane of bronchiolar cells, type II pneumocytes and alveolar macrophages (14,15). The postmortem study of H5N1-infected patients has recently been published for the first time (16).

In the present study, we describe the histopathological findings from three fatal cases of H5N1 infection from the National Hospital of Pediatrics in Hanoi, Vietnam. The detailed clinical findings of Case 1 and Case 2 have been described previously (5). On admission, all patients presented with fever, cough, and dyspnea, and H5N1 virus was detected in tracheal fluids by reverse-transcriptase polymerase chain reaction (RT-PCR) before death occurred. The duration of the disease in Case 1, 6 days, was much shorter than in the other two cases (Table 1). Small pieces of lung tissues in the lower respiratory tract were necropsied and histological and immunohistochemical examinations were carried out on formalin-fixed and paraffin-embedded lung tissues.

The hematoxylin and eosin-stained lung sections of Case 1 demonstrated typical histological features of diffuse alveolar damage (DAD) with an exudative phase (Fig. 1a). Eosinophilic hyaline membrane was found on alveolar ducts and on alveoli. The alveolar space was filled with proteinaceous exudates containing erythrocytes, macrophages, and cell debris. The alveolar septa were thickened by edema with mild inflammatory infiltration, consisting of lymphocytes and macrophages. In Cases 2 and 3, hyaline membrane formation was focally found, and the proliferation of fibroblasts in the interstitial space was marked in comparison to Case 1. Mild interstitial inflammation and proliferation of type II pneumocytes with bizarre and cuboidal features were observed (Fig. 1c), indicating that Cases 2 and 3 were in the proliferative (repair) phase of DAD. Squamous cell metaplasia in the bronchiolar epithelium was also observed (Fig. 1d). Focal accumulation of neutrophils in the alveolar space was found in Case 3, suggesting pulmonary bacterial infection. These histological features were similar to those reported previously in fatal human H5N1 influenza A virus-infected cases (4,8,10,11).

To detect the influenza A virus antigen, the sections were immunostained with an avidin-biotin complex immunoperoxidase method (LSAB2 kit/HRP/DAB; Dako Cytomation, Copenhagen, Denmark) using a mouse monoclonal antibody against InfA-NP (17). Positive signals for InfA-NP were detected in 6 of 6 blocks of lung tissue from Case 1, whereas they were not found in those from Case 2 or 3. The signals were found mainly in alveolar epithelial cells and in interstitial cells (Fig. 1b). The many positive cells were interpreted as type II pneumocytes and/or alveolar macrophages, but the positive cell presented in the inset in Fig. 1b was considered to be a type I pneumocyte based on its histological location and morphology. H5N1-RNA was also detected by real-time RT-

*Corresponding author: Mailing address: Chiba University Graduate School of Medicine, Inohana 1-8-1, Chuo-ku, Chiba 260-8670, Japan. Tel: +81-43-221-0831, Fax: +81-43-221-0832, E-mail: ksuzuki@faculty.chiba-u.jp

**Deceased after the contribution of this study.

Table 1. Histopathological findings in the lung of H5N1 fatal cases in Vietnam

Case	Age (y)/ Sex	Days from onset to death	Histology in lung sections	RT-PCR for H5N1 (tracheal fluids)	RT-PCR for H5N1 (paraffin-embedded sections of lung)	Immunohistochemistry for InfA-NP antigen and co-localization with cell marker proteins
1[1]	12/F	6	DAD with an exudative phase, Hyaline membrane formation Hemmorhagic necrosis	Positive	Positive	Positive for InfA-NP antigen, and colocalized with AE1/AE3, EMA, SPA, SPD, CD68, CD34
2[2]	5/M	17	DAD with a proliferative (repair) phase Hyaline membrane formation	Positive	Negative	Negative for InfA-NP antigen
3	4/M	16	DAD with a proliferative (repair) phase Hyaline membrane formation Microabscess	Positive	Negative	Negative for InfA-NP antigen

[1]: Patient 1 in Ref (5).
[2]: Patient 2 in Ref (5).
M, male; F, female; DAD, diffuse alveolar damage; InfA-NP, influenza virus A nucleoprotein; EMA, epithelial membrane antigen; SPA, surfactant protein A; SPD, surfactant protein D.

Table 2. Antibodies used for double immunofluorescence staining

Antigen	Antibody type	Stained cells	Source
cytokeratin (AE1/AE3)	mouse monoclonal	epithelial cell of bronchiole	Dako
epithelial membrane antigen (EMA)	mouse monoclonal	epithelial cell	Dako
surfactant apoprotein A (SPA)	mouse monoclonal	type II alveolar pneumocyte	Dako
surfactant apoprotein D (SPD)	rabbit polyclonal	type II alveolar pneumocyte	Chemicon[1]
CD68 (KP1)	mouse monoclonal	alveolar macrophage	Dako
CD68 (PG-M1)	mouse monoclonal	alveolar macrophage	Dako
CD34	mouse monoclonal	endothelial cell	Immunotech[2]
influenza A virus nucleoprotein	mouse monoclonal	influenza A virus infected cell	in-house Ref. (17)
influenza A virus nucleoprotein	rabbit polyclonal	influenza A virus infected cell	in-house Ref. (17)

[1]: Chemicon, Temecula, Calif., USA.
[2]: Immunotech, Marseille, France.

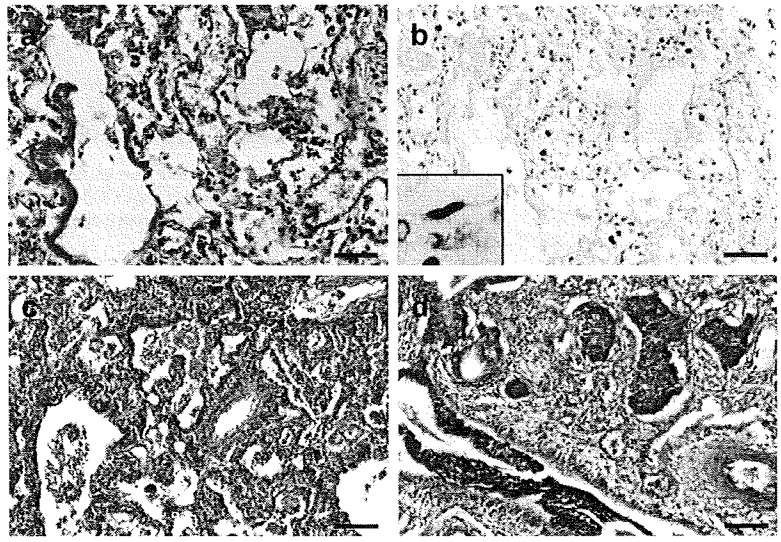

Fig. 1. Hematoxylin and eosin stainings and immunohistochemistry for influenza virus A nucleoprotein (InfA-NP) in Case 1. (a) Hyaline membrane formation is observed on the alveolar walls. In the interstitial space, edema and mild inflammatory cell infiltrates are observed (Case 1). (b) InfA-NP antigens are detected in alveolar epithelial cells and in the interstitial space. InfA-NP-positive, type I pneumocyte is indicated in the inset. (c) Mild interstitial inflammation and proliferation of type II pneumocytes with bizarre and cuboidal features were observed (Case 3). (d) Squamous cell metaplasia in the bronchiolar epithelium was also observed (Case 2). Scale bar = 100 μm.

PCR in paraffin-embedded lung sections from Case 1 only (18). In DAD with a proliferative phase, as in Cases 2 and 3, viral antigens and nucleic acids were not detected.

To characterize virus-infected cells, confocal laser scanning microscopy was used to visualize double immunofluorescence staining for InfA-NP and for cell-type specific marker proteins of epithelial cells, macrophages, and endothelial cells. The antibodies used are shown in Table 2. Alexa Fluor 568-conjugated anti-mouse or anti-rabbit IgG (Molecular Probes, Eugene, Oreg., USA) and Alexa Fluor 488-conjugated anti-rabbit or anti-mouse IgG (Molecular Probes) were used as secondary antibodies. InfA-NP signals were detected most

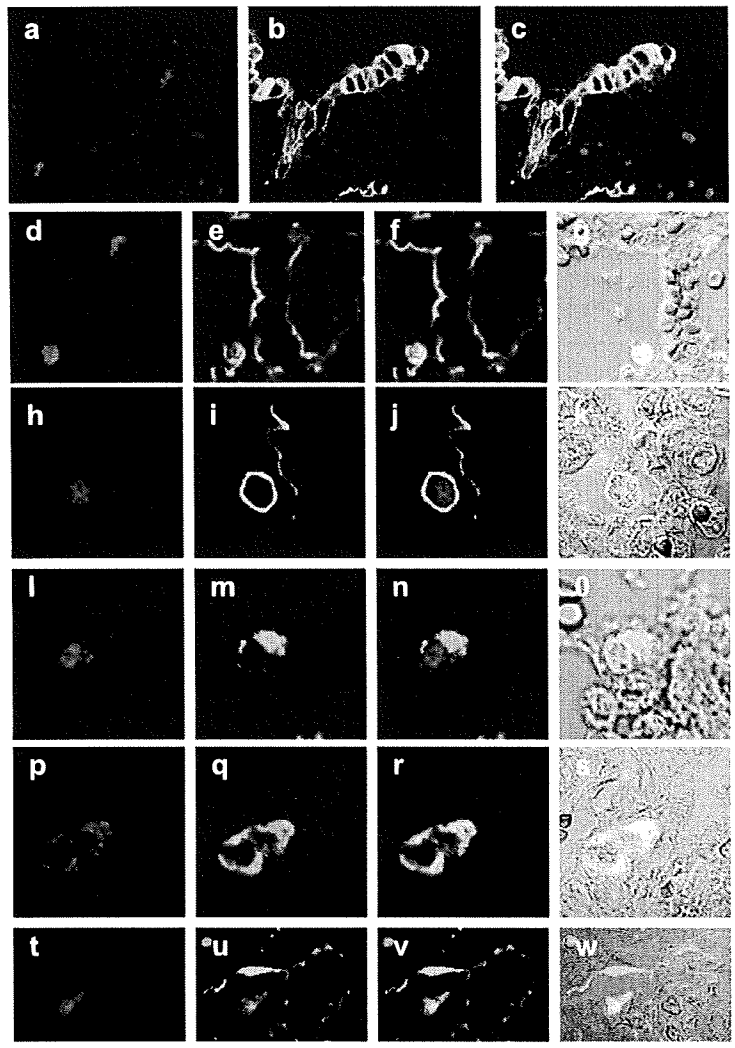

Fig. 2. The phenotype of influenza virus A nucleoprotein (InfA-NP) positive cells. InfA-NP immunoreactivity (a, d, h, l, p, t) (red color) and cytokeratin (b), EMA (e), SPD (i), CD68 (Kp1) (m), CD68 (PGM-1) (q) or CD34 (u) immunoreactivity (green color). Co-localization is presented respectively (c, f, j, n, r, v). Differential interference contrast (DIC) images are also shown (g, k, o, s, w). Original magnifications, ×400.

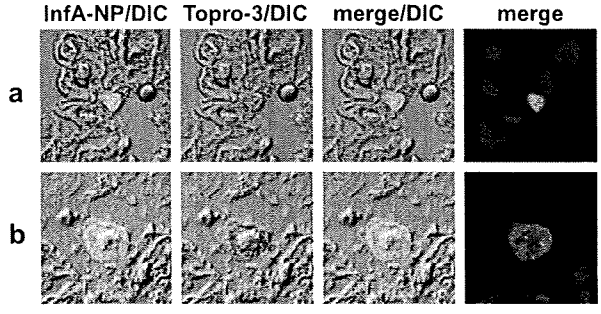

Fig. 3. Immunofluorescence staining of InfA-NP antigen in infected epithelial cells. InfA-NP immunoreactivity (red color), TO-PRO-3 nucleic acid staining (blue color) and merged images (pink color) are shown. Some were analyzed with differential interference contrast (DIC) images. The InfA-NP antigen was localized in nuclei (a) or in cytoplasm (b). Original magnifications, ×400.

frequently in epithelial (EMA-positive) cells. They were also detected in AE1/AE3, SPD, SPA, and CD68-positive cells (Fig. 2), indicating that H5N1 virus antigens were present predominantly in the epithelial cells in terminal bronchioles and alveoli, mainly in type II alveolar pneumocytes and in alveolar macrophages. A few H5N1 virus-infected type I pneumocytes were also suggested by double-positive staining for InfA-NP and for EMA, in combination with distinctive morphology. Although the number was very few, the InfA-NP signal was also detected in CD34-positive cells, suggesting that the H5N1 had infected some CD34-positive endothelial cells. Further investigation will be necessary to confirm the H5N1 infection of human endothelial cells, as has been observed in the endothelial cells of chickens and other birds (19). The localization of InfA-NP antigen within the cell was determined by counterstaining with TO-PRO-3 nucleic acid staining (Molecular Probes). Some InfA-NP signals were detected in nuclei (Fig. 3a) and others were detected in the cytoplasm (Fig. 3b). Histologically, in the early phase of infection, InfA-NP antigen was localized in the nucleus, while in the late phase of infection, InfA-NP antigen was localized in the cytoplasm (20). These observations suggested that viruses were in the proliferative stage in the early phase of H5N1 infection. The histopathological data

are summarized in Table 1.

Avian influenza viruses have been found to preferentially bind to sialic acid-α-2,3-Gal (SAα2-3)-linked oligosaccharides, while human influenza viruses were found to bind to SAα2-6-linked oligosaccharides (21), although these findings were made in vitro or ex vivo experiments. As an in vivo examination, we performed an analysis with the double-staining technique using a monoclonal antibody against InfA-NP in combination with either biotinylated *Maackia amurensis* agglutinin (MAA) lectin (Vector Laboratories, Burlingame, Calif., USA) which is specific for SAα2-3-linked oligosaccharides, or with *Sambucus nigra* agglutinin (SNA) lectin (EY Laboratories, San Mateo, Calif., USA), which is specific for SAα2-6-linked oligosaccharides. In the alveoli, many cells were not stained by SNA lectin but were stained by MAA lectin, suggesting that they express SA α 2-3-linked oligosaccharides, as found in previous reports (21). Unexpectedly, the InfA-NP-positive cells were not double-stained by MAA lectin.

Although the materials were restricted to small pieces of lung tissue in the lower respiratory tract, the evidence in the present study showed that several types of cells in the lung, namely type I and type II alveolar pneumocytes, epithelial cells in terminal bronchioles, macrophages in the alveolar space and CD34-positive endothelial cells in the interstitial tissues, were involved in the disease. The evidence in Case 1, the case with H5N1 infection who died on day 6 after onset, strongly suggests that H5N1 may infect the epithelial cells of alveolar tissues in the early clinical phase and can thereafter be transmitted to adjacent cells. The dissemination of infection among these cells was supposed to be accompanied by the release of pro-inflammatory cytokines from the infected alveolar macrophages (4,10,12), resulting in rapid progression from DAD with an exudative phase to that with a proliferative phase.

ACKNOWLEDGMENTS

This study was supported in part by grants of Ministry of Education, Culture, Sports, Science and Technology of Japan and Ministry of Health, Labour and Welfare of Japan.

REFERENCES

1. Subbarao, K., Klimov, A., Katz, J., et al. (1998): Characterization of avian influenza A (H5N1) virus isolated from a child with a fatal respiratory illness. Science, 279, 393-396.
2. Claas, E.C.J., Osterhaus, A.D.M.E., van Beek, R., et al. (1998): Human influenza A H5N1 virus related to a highly pathogenic avian influenza virus. Lancet, 351, 472-477.
3. To, K.F., Chan, P.K.S., Chan, K.F., et al. (2001): Pathology of fatal human infection associated with avian influenza A H5N1 virus. J. Med. Virol., 63, 242-246.
4. Peiris, J.S.M., Yu, W.C., Leung, C.W., et al. (2004): Re-emergence of fatal human influenza A subtype H5N1 disease. Lancet, 363, 617-619.
5. Hien, T.T., Liem, N.T., Dung, N.T., et al. (2004): Avian influenza A (H5N1) in 10 patients in Vietnam. N. Engl. J. Med., 350, 1179-1188.
6. Ungchusak, K., Auewarakul, P., Dowell, S.F., et al. (2005): Probable person-to-person transmission of avian influenza (H5N1). N. Engl. J. Med., 352, 333-340.
7. Chokephaibulkit, K., Uiprasertkul, M., Puthavathana, P., et al. (2005): A child with avian influenza A (H5N1) infection. Pediatr. Infect. Dis. J., 24, 162-166.
8. Chotpitayasunondh, T., Ungchusak, K., Hanshaoworakul, W., et al. (2005): Human disease from influenza A (H5N1), Thailand, 2004. Emerg. Infect. Dis., 11, 1036-1041.
9. World Health Organization. Confirmed human cases of avian influenza A (H5N1). Online at <http://www.who.int/csr/disease/avian_influenza/country/en/>. Accessed 4 September 2007.
10. Uiprasertkul, M., Puthavathana, P., Sangsiriwut, K., et al. (2005): Influenza A H5N1 replication sites in humans. Emerg. Infect. Dis., 11, 201-209.
11. Ng, W.F., To, K.F., Lam, W.W.L., et al. (2006): The comparative pathology of severe acute respiratory syndrome and avian influenza A subtype H5N1–a review. Hum. Pathol., 37, 381-390.
12. Uiprasertkul, M., Kitphati, R., Puthavathana, P., et al. (2007): Apoptosis and pathogenesis of avian influenza A (H5N1) virus in humans. Emerg. Infect. Dis., 13, 708-712.
13. Nicolls, J.M., Chan, M.C.W., Chan, W.Y., et al. (2007): Tropism of avian influemza A (H5N1) in the upper and lower respiratory tract. Nat. Med., 13, 147-149.
14. Riel, D.V., Munster, V.J., de Wit, E., et. al. (2006): H5N1 virus attachment to lower respiratory tract. Science, 399, 312.
15. Riel, D.V., Munster, V.J., de Wit, E., et al. (2007): Human and avian influenza viruses target different cells in the lower respiratory tract of humans and other mammals. Am. J. Pathol., 171, 1215-1222.
16. Gu, J., Xie, Z., Liu, J., et.al. (2007): H5N1 infection of the respiratory tract and beyond: a molecular pathology study. Lancet, 370, 1137-1145.
17. Chen, Z., Sahashi, Y., Matsuo, K., et al. (1998): Comparison of the ability of viral protein-expressing plasmid DNAs to protect against influenza. Vaccine, 16, 1544-1549.
18. Ng, E.K.O., Cheng, P.K.C., Ng, A.Y.Y., et al. (2005): Influenza A H5N1 detection. Emerg. Infect. Dis., 11, 1303-1305.
19. Lee, C.W., Suarez, D.L., Tumpey, T.M., et al. (2005): Characterization of highly pathogenic H5N1 avian influenza A viruses isolated from south Korea. J. Virol., 79, 3692-3702.
20. Nishimura, H., Itamura, S., Iwasaki, T., et al. (2000): Characterization of human influenza A (H5N1) virus infection in mice: neuro-, pneumo- and adipotropic infection. J. Gen. Virol., 81, 2503-2510.
21. Shinya, K., Ebina, M., Yamada, S., et al. (2006): Avian flu: influenza virus receptors in the human airway. Nature, 440, 435-436.

Available online at www.sciencedirect.com
ScienceDirect
Current Opinion in Immunology
ELSEVIER

Initiation and maintenance of Th2 cell identity

Toshinori Nakayama and Masakatsu Yamashita

T helper type 2 (Th2) cells produce IL-4, IL-5, and IL-13 and play an important role in humoral immunity and allergic reactions. During Th2 cell differentiation, naïve CD4 T cells acquire 'Th2 cell identity', that is, the capability to produce selectively a large amount of Th2 cytokines. Th2 cell identity is maintained in memory Th2 cells. Significant advances in understanding of the molecular requirement for these processes have been made. The expression of GATA3, a master transcription factor for Th2 cell differentiation, is uniquely regulated by several distinct mechanisms. Molecular analyses of memory Th2 cells revealed that cell survival and the maintenance of Th2 cell function are epigenetically regulated by various nuclear factors, including *Polycomb* and *Trithorax* molecules.

Address
Department of Immunology, Graduate School of Medicine, Chiba University, 1-8-1 Inohana, Chuo-ku, Chiba 260-8670, Japan

Corresponding author: Nakayama, Toshinori (tnakayama@faculty.chiba-u.jp)

Current Opinion in Immunology 2008, **20**:265–271

This review comes from a themed issue on
Lymphocyte Activation
Edited by Anjana Rao and Kathryn Calame

Available online 22nd May 2008

0952-7915/$ – see front matter

DOI 10.1016/j.coi.2008.03.011

Introduction

It has been established that effector helper T (Th) cells can be categorized into at least four subsets, Th1, Th2, Th17, and T regulatory (Tr) cells. Th1 cells produce large amounts of IFNγ and direct cell-mediated immunity against intracellular pathogens. Th2 cells produce IL-4, IL-5, and IL-13 and are involved in the humoral immunity and allergic reactions. Recently identified Th17 cells are crucial in certain autoimmune diseases. Tr cells are known to suppress various immune responses including autoimmune responses. Several transcription factors that control the differentiation and the function of these Th cell subsets have been identified. Among them, GATA3 appears to be a master transcription factor for Th2 cell differentiation [1,2], T-bet for Th1 [3], RORγt for Th17 [4], and FoxP3 for naturally occurring Tr [5].

Th1/Th2 responses are induced by antigen-specific effector and memory Th1/Th2 cells. Figure 1 illustrates the cellular processes that are required for the generation of functional memory Th1/Th2 cells from effector Th1/Th2 cells. After antigen recognition by TCR, naïve CD4 T cells undergo clonal expansion and differentiate into effector Th1/Th2 cells within a couple of weeks. After antigen clearance, most of the effector Th1/Th2 cells are thought to undergo apoptotic cell death at the contraction phase [6,7]. Some of the effector cells, however, escape cell death, differentiate into memory type Th1/Th2 cells, and survive for a long time *in vivo*. Several processes, including cell survival/escape from cell death, proliferation/homeostatic proliferation, and the maintenance of Th1/Th2 cell function are all required for the successful generation of functional memory type Th1/Th2 cells. The idea of memory stem cells is also considered, but this has not been experimentally proven at this time.

In this review, we present recent findings that provide new insights in our understanding of the molecular mechanisms governing the acquisition and the maintenance of Th2 cell identity.

Expression of GATA3 is required for the initiation and the maintenance of Th2 responses

The initiation of Th2 cell differentiation is dependent on TCR-mediated signaling, and the IL-4 receptor-mediated STAT6 activation and subsequent upregulation of GATA3 transcription. Enforced expression of GATA3 in developing Th1 cells was sufficient to cause the induction of IL-4 producing Th2 type cells in the absence of STAT6, indicating that GATA3 is a downstream target of the IL-4/STAT6 signaling pathway and a master transcription factor for Th2 cell differentiation [1,2]. During Th2 cell differentiation, GATA3 plays a central role in the induction of chromatin remodeling of the Th2 cytokine gene loci (Figure 2a) [8–11]. The differentiated effector Th2 cells now acquire 'Th2 cell identity', that is, the capability to produce selectively a large amount of Th2 cytokines upon TCR re-stimulation. GATA3 is also known to act as a transcription factor for the Th2 cytokine genes, particularly for IL-5 and IL-13. In order to investigate whether GATA3 plays a role in the maintenance of the Th2 cell identity, we established a gene-depletion system in primary *in vitro* differentiated Th2 cells using a site-specific recombination reaction [12]. The depletion of the GATA3 gene resulted in a substantial decrease in the production of Th2 cytokines (IL-4, IL-5, and IL-13) and a significant increase in IFNγ. Two other groups using GATA3 conditional knockout mice demonstrated an important role of GATA3 in Th2 responses *in vivo* [13,14]. *In vivo* deletion of the GATA3

Figure 1

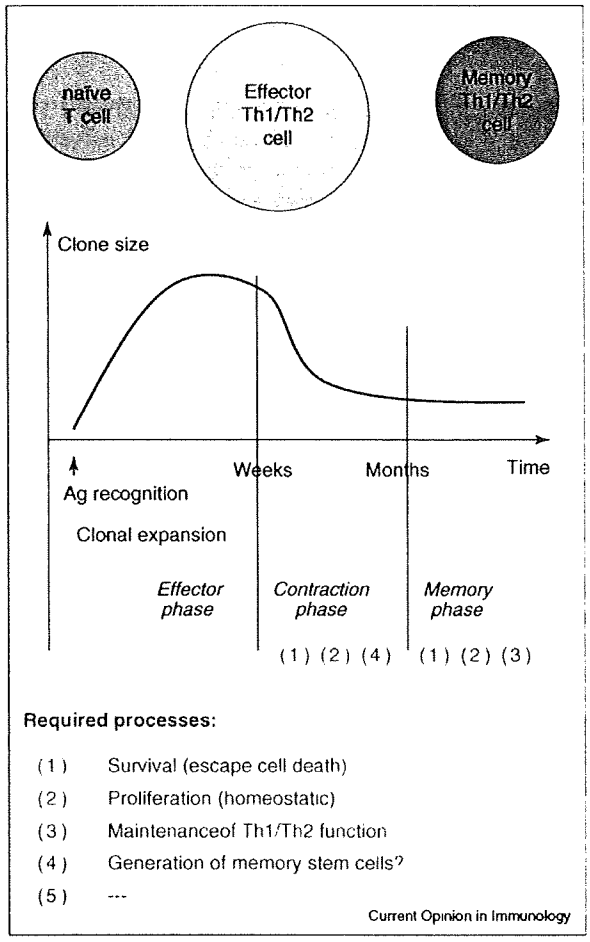

Cellular processes required for the generation of functional memory Th1/Th2 cells. Details are described in the text.

gene using OX40-Cre eliminated Th2 responses and allowed the development of IFN-γ producing cells in mice infected with *Nippostrongylus brasiliensis*, suggesting that GATA3 serves as a principal switch in determining Th1/Th2 response [13]. The requirement of GATA3 expression in the optimal Th2 cytokine production is also indicated in another line of GATA3 conditional knockout mice [14]. Interestingly, however, the established histone modifications (histone H3-K9/14 hyper-acetylation and H3-K4 hyper-methylation) at the Th2 cytokine gene loci were not apparently affected by the depletion of the GATA3 gene in the *in vitro* differentiated Th2 cells [12]. Thus, once the Th2 cell identity is established, GATA3 may not be largely involved in the regulation of chromatin status, but still plays an important role as a transcription factor for the Th2 cytokine genes (Figure 2b).

Regulation of GATA3 expression

IL-4/STAT6-mediated signals are required for the upregulation of GATA3 transcription in developing Th2 cells, while the basal expression of GATA3 in naïve CD4 T cells is not dependent on STAT6 activation. In thymocytes, GATA3 expression was shown to be controlled by c-Myb [15], E2A [16], and Notch signaling [17]. Notch signaling was reported to regulate GATA3 expression also in peripheral CD4 T cells [18••,19••]. Notch1 ICD (intra cellular domain) and its signaling component, RBP-J, bind to the upstream promoter of GATA3 and induce transcription of GATA3 involving exon 1a. IL-4/STAT6 signaling also induces the GATA3 transcription from exon 1a. Although the relationship between Notch1-mediated signaling and IL-4/STAT6 signaling remains unclear at this time, the Notch1 ICD/RBP-J complex may substitute for STAT6 during Th2 cell differentiation, or the IL-4/STAT6 activation may control the accessibility of the Notch-signaling complex to the GATA3 gene promoter. In fact, Notch was previously reported to play an important role in Th1 cell differentiation [20,21] and both Th1/Th2 cell differentiation [22]. Ectopic expression of Notch1 ICD in CD4 T cells resulted in Th1 cell differentiation, and the suppression of Notch signaling by a γ-secretase inhibitor blocked Th1 cell differentiation [20]. In this report, the Notch ICD/RBP-J complex was demonstrated to directly regulate the T-bet promoter. Thus, Notch/RBP-J signaling may play various roles in the regulation of Th1 and Th2 cell differentiation, and further investigation will be required for understanding the precise role of the Notch signaling pathway.

An important role for NF-κB activation in the expression of GATA3 was originally reported in the allergic asthma model [23]. Recently, Notch1 and Notch3 were reported to augment the NF-κB activity in T cells and thymocytes, respectively [24,25]. Notch1 ICD directly interacts with the NF-κB complex to facilitate its nuclear retention, whereas Notch3 binds IKKα and maintains NF-κB activation through the p52/RelB pathway. A zinc finger C2H2 type transcriptional repressor, Schnurri-2 (Shn-2) was reported to suppress the expression of GATA3 through the inhibition of NF-κB activity [26]. In the absence of Shn-2, hyper-activation of NF-κB is induced in naïve and developing Th2 cells, and the increased expression of GATA3 and augmented Th2 responses were observed [26]. In addition, protein kinase C (PKC) θ appears to regulate NF-κB activation and GATA3 expression. In PKCθ-deficient CD4 T cells, the expression of GATA3 was severely impaired and Th2 cytokine production decreased [27]. Moreover, PKCθ was reported to be a downstream target of Notch3 [28]. Thus, the expression of GATA3 appears to be controlled by NF-κB activation in thymocytes and peripheral CD4 T cells.

A high level ubiquitination and efficient proteasome-dependent degradation of GATA3 molecules in primary

Figure 2

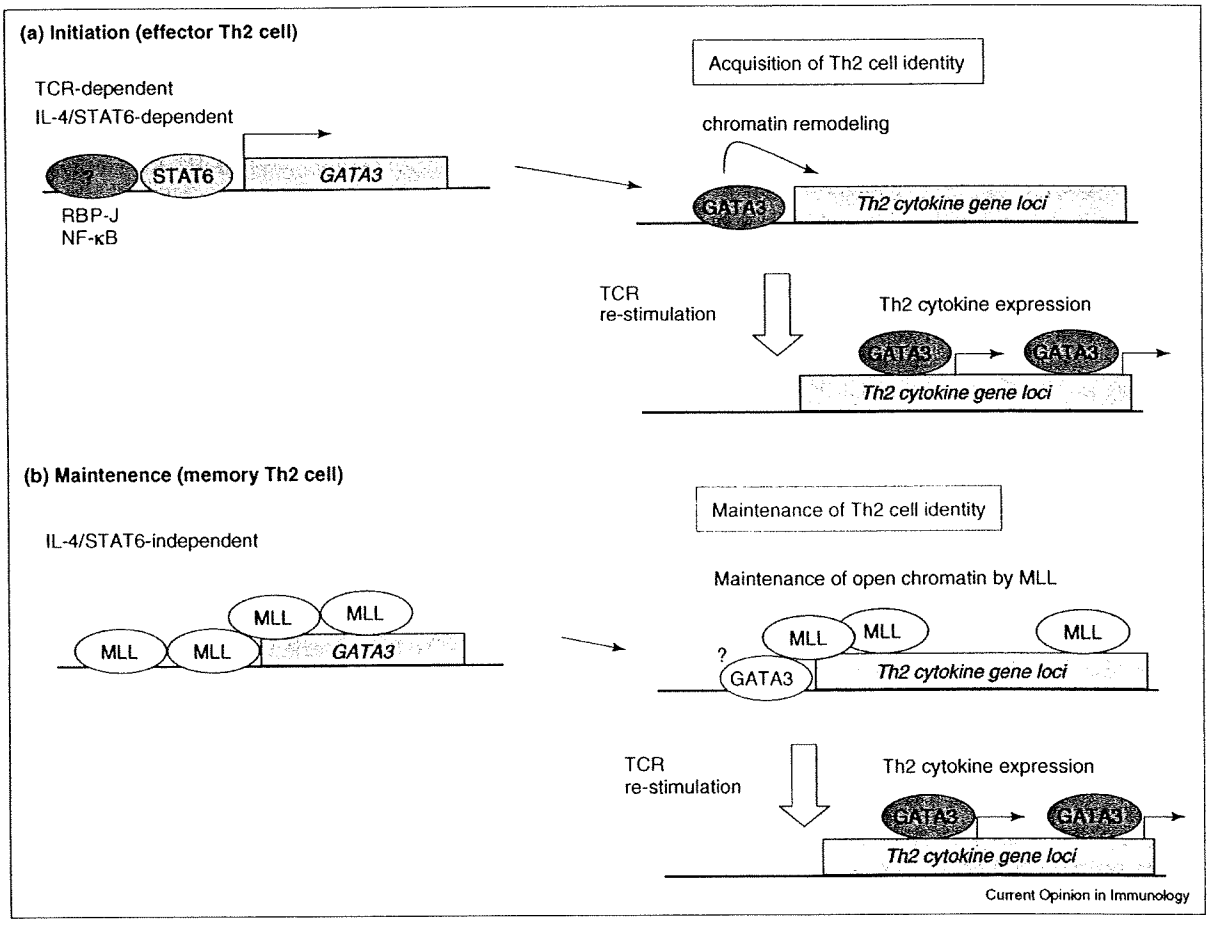

Molecular requirement for the initiation and the maintenance of Th2 cell identity. **(a)** The initiation of Th2 cell differentiation is dependent on TCR-mediated signaling and IL-4-receptor-mediated STAT6 activation, and subsequent upregulation of GATA3 transcription. GATA3 plays a central role in the induction of chromatin remodeling of the Th2 cytokine gene loci. GATA3 is also known to act as a transcription factor for the Th2 cytokine genes. **(b)** Once Th2 cell identity is established, GATA3 may not be largely involved in the regulation of chromatin status, but still plays an important role as a transcription factor for the Th2 cytokine genes. In memory Th2 cells, a histone H3-K4 methyltransferase, MLL binds to the GATA3 gene locus and Th2 cytokine gene loci to maintain the hyper-methylation status of H3-K4. MLL histone H3-K4 methyltransferase complex may contribute to IL-4/STAT6-independent maintenance of Th2 cell identity in memory Th2 cells. Once memory Th2 cells are stimulated through TCR, GATA3-dependent Th2 cytokine gene expression is induced.

CD4 T cells have been demonstrated [29]. Mdm2 was found to physically interact with GATA3 and induce multi-ubiquitination and subsequent degradation, indicating that Mdm2 acts as an E3 ligase for GATA3. Interestingly, the ubiquitin/proteasome-dependent degradation of GATA3 protein was counteracted by the TCR-mediated activation of the ERK-MAPK cascade [29]. This may explain the requirement for TCR signals, in addition to the IL-4/STAT6-dependent signal, for the induction of Th2 cell differentiation following GATA3 mRNA expression. Thus, the expression of GATA3 is also controlled at the protein level.

Epigenetic regulation of Th2 cytokine expression

Chromatin structure is an important determinant of gene activation and silencing that is regulated by various epigenetic processes. Changes in chromatin structure at the Th2 cytokine (IL-4/IL-5/IL-13) gene loci occur during Th2 cell differentiation. The chromosome conformation capture (3C) assay is a new technique to analyze the changes of chromatin configuration. Spilianakis and Flavell applied this technique to the Th2 cytokine gene loci and demonstrated that a recently identified Th2 LCR (locus control region) [30,31] is required for T-cell-specific hub formation [32]. GATA3

and STAT6 are required for the establishment and/or maintenance of the interactions [32]. Targeted deletion of the Th2-specific LCR (LCR-C/RHS7 HS) was associated with decreased long-range interchromosomal interactions between this LCR and the promoters of the Th2 cytokine genes [33]. More recently, Cai *et al.* reported that TCR-mediated induction of SATB1 (special AT-rich sequence binding protein 1) was required for the coordinated expression of Th2 cytokines [34••]. SATB1 organizes cell-type-specific nuclear architecture by anchoring specialized DNA sequences and recruiting chromatin remodeling factors, and controls various gene transcriptions. After TCR stimulation, SATB1 was rapidly induced and bound to several specific regions (CNS1, CNS2, etc.) at the Th2 cytokine gene loci including the RAD50 and KIF3A genes. A 3C assay and ChIP-loop assay [34••] revealed that SATB1 is crucial for the formation of higher order chromatin structure around the Th2 cytokine gene loci and regulates the accessibility of RNA polymerase II, Brg1, and c-Maf.

In Th1 cells, the stable inhibition of the expression of IL-4 has been attributed to epigenetic regulation. DNA hypersensitive (HS) site IV is located at the 3′ end of the IL-4 gene locus and plays a crucial role in the Th1-specific silencing of the expression of IL-4 [35]. Runx3 has emerged as a potential regulator of the HS IV-mediated IL-4 gene silencing in Th1 cells [36•,37•]. Runx3 was upregulated during Th1 cell differentiation in a T-bet-dependent manner, and Runx3 and T-bet cooperatively bound to the IFN-γ promoter and the IL-4 silencer. Th1 cells that lack the HS IV region were less sensitive to the repression of IL-4 by T-bet and Runx3 [36•]. Interestingly, in naïve CD4 T cells, Runx1 complex binds to the IL-4 silencer instead of Runx3. The overexpression of GATA3 in Th1 cells induced the dissociation of the Runx complex from the IL-4 silencer [37•]. An analysis on the chromatin configuration around the Th2 cytokine loci may provide a clearer view of the molecular events underlying the Runx-dependent repression of the IL-4 gene in Th1 cells.

Maintenance of the expression of the GATA3 gene locus and Th2 cytokine gene loci by a *Trithorax* group gene product, MLL

Once a high level expression of GATA3 is induced in *in vitro* differentiated Th2 cells via the activation of IL-4/STAT6-mediated signaling, the high level GATA3 expression is maintained in an IL-4-independent manner (Figure 2b). It is known that the dimethylation and trimethylation of histone H3-K4 are associated with the transcriptionally active status of chromatin [38]. In *in vitro* established Th2 cells, histone H3-K4 methylation and H3-K9/14 acetylation of the upstream region of GATA3 promoter (between exon 1a and exon 1b) are detected [39••]. A genome-wide analysis of the H3-K4 methylation pattern in human and mouse fibroblast and tumor cell lines was previously reported [40]. However, the molecular dynamics governing the changes in H3-K4 methylation during cell differentiation has not been well analyzed. Since the expression of GATA3 is crucial for inducing Th2 responses, it is important to study the mechanisms governing the induction and the maintenance of H3-K4 methylation at the GATA3 gene locus.

MLL, mixed lineage leukemia is a member of the *Trithorax* group gene. MLL possesses a histone methyltransferase activity for H3-K4, and forms a huge protein complex containing RNA polymerase II [41]. Figure 3 illustrates the proposed MLL complex [41] (MY and TN, unpublished observation). Recently, we have reported a crucial role for MLL for the maintenance of the expression of the GATA3 gene [39••]. A substantial decrease in the transcription of GATA3 accompanied by decreased methylation levels of H3-K4 at the GATA3 gene locus was detected in MLL-knockdown Th2 cell lines and in *in vivo* generated memory Th2 cells with an *MLL* heterozygous background. Thus, the maintenance of transcriptional expression of GATA3 in established Th2 cells including memory Th2 cells is epigenetically regulated by MLL (Figure 2b, left).

The histone modifications including histone H3-K9 hyper-acetylation at the IL-4 gene locus were also maintained in an IL-4-independent manner in memory Th2 cells. In addition to the GATA3 gene locus, MLL is also found to be involved in the maintenance of activated chromatin status at the Th2 cytokine gene loci (Figure 2b, right) [39••]. The direct binding of MLL at specific regions on the IL-4 and IL-13 gene loci was detected. Th2 cytokine production was severely reduced in MLL-knockdown Th2 cell lines and MLL heterozygous memory Th2 cells accompanied by decreased levels of H3-K9/14 acetylation and H3-K4 methylation.

Figure 3

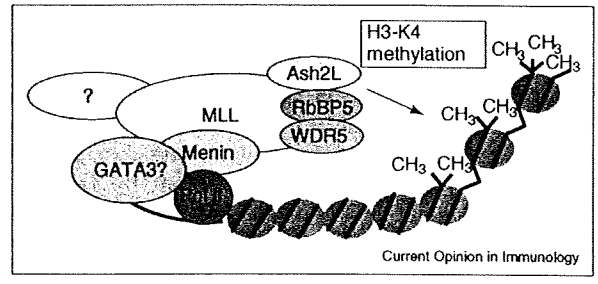

A proposed MLL complex. MLL is reported to be associated with Ash2L, RbBP5, WDR5, and Menin. Ash2L is a *Trithorax* group molecule. RbBP5 and WDR5 are WD40 repeat-containing protein. Menin is a *MEN1* tumor suppressor gene product. Several other molecules appear to be associated with MLL.

Maintenance of memory Th2 cell numbers

In order to establish sufficient memory Th1/Th2 cell responses, effector Th1/Th2 cells must escape apoptotic cell death and survive at the contraction phase (Figure 1). In a series of studies on the role of Shn-2 in the CD4 T cell immunity, we have found that Shn-2 is required for the generation of sufficient numbers of both memory Th1 and Th2 cells [42•]. The expression levels of Shn-2 were high in naïve CD4 T cells, but they were decreased after TCR stimulation, and increased again in memory Th1/Th2 cells, particularly in memory Th2 cells. Shn-2-deficient effector Th1 and Th2 cells showed hyper-activation of the NF-κB signaling pathway and tended to die at the contraction phase, partly owing to the increased susceptibility to apoptosis via the Fas/FasL pathway. Thus, after antigen clearance, the successful generation of memory Th1/Th2 cells appears to require Shn-2-mediated deactivation of the NF-κB signaling pathway at the contraction phase.

Memory T cells have several features associated with stem cells, and the similarity of the gene expression patterns between memory T/B cells and long-term hematopoietic stem cells was reported [43]. The *Polycomb* group gene *Bmi1* has been implicated in the maintenance of hematopoietic, neural, and cancer stem cells. We recently found that Bmi1 supports memory Th1/Th2 cell survival via the repression of the expression of the *Noxa* gene [44]. Noxa is a member of the proapoptotic BH3 only protein. Although Bmi1 was reported to promote cell proliferation, cell survival and stem cell self-renewal by the repression of the *Ink4a/Arf* gene locus, Bmi1-mediated regulation of the expression of the *Noxa* gene and the survival of memory CD4 T cells were found to be *Ink4a/Arf*-independent. Although less is known about the molecules that control the cell survival of memory CD4 T cells, further analyses on the nuclear factors that are preferentially expressed in memory T cells may provide new insights in our understanding of the generation and the maintenance of memory Th2 responses.

Conclusion

In the past few years, new insights into the molecular requirement for the epigenetic regulation of Th2 cell identity have emerged. A role for GATA3 expression has been more highlighted both in the initiation and the maintenance of Th2 cell identity. GATA3 may control the Th2 cytokine gene expression in a variety of ways through the association with distinct functional nuclear complexes including Polycomb, Trithorax, HAT, HDAC, Pol II, and those containing chromatin modifying factors such as SATB1. The elucidation of the nature of GATA3 complexes, particularly that of cell-type-specific differences of the GATA3 complex may provide a more comprehensive view of the regulation of Th2 cell identity. *Polycomb* and *Trithorax* group gene products counteract each other in function during the development in *Drosophila* and mammals. The analyses of precise molecular actions of these two interesting molecules in the initiation and the maintenance of Th2 cell identity would also be also intriguing.

Acknowledgements

The authors are grateful to Dr Ralph T Kubo for valuable comments during the preparation of this manuscript. We thank former and current staff members, Dr Motoko Y Kimura, Dr Aki Hasegawa, and Dr Hiroyuki Hosokawa who contributed to the primary work. We apologize to those researchers in the field whose relevant publications we could not cite because of space limitations. This work was supported by grants from the Ministry of Education, Culture, Sports, Science and Technology (Japan) (Grants-in-Aid for: Scientific Research in Priority Areas #17016010 and #17047007; Scientific Research B #17390139, Scientific Research C #18590466), the Ministry of Health, Labor and Welfare (Japan).

References and recommended reading

Papers of particular interest, published within the annual period of the review, have been highlighted as:

- • of special interest
- •• of outstanding interest

1. Ansel KM, Djuretic I, Tanasa B, Rao A: **Regulation of Th2 differentiation and Il4 locus accessibility**. *Annu Rev Immunol* 2006, **24**:607-656.
2. Mowen KA, Glimcher LH: **Signaling pathways in Th2 development**. *Immunol Rev* 2004, **202**:203-222.
3. Szabo SJ, Sullivan BM, Peng SL, Glimcher LH: **Molecular mechanisms regulating Th1 immune responses**. *Annu Rev Immunol* 2003, **21**:713-758.
4. Ivanov II, McKenzie BS, Zhou L, Tadokoro CE, Lepelley A, Lafaille JJ, Cua DJ, Littman DR: **The orphan nuclear receptor RORgammat directs the differentiation program of proinflammatory IL-17+ T helper cells**. *Cell* 2006, **126**:1121-1133.
5. Sakaguchi S, Ono M, Setoguchi R, Yagi H, Hori S, Fehervari Z, Shimizu J, Takahashi T, Nomura T: **Foxp3+ CD25+ CD4+ natural regulatory T cells in dominant self-tolerance and autoimmune disease**. *Immunol Rev* 2006, **212**:8-27.
6. Marrack P, Kappler J: **Control of T cell viability**. *Annu Rev Immunol* 2004, **22**:765-787.
7. Stockinger B, Kassiotis G, Bourgeois C: **CD4 T-cell memory**. *Semin Immunol* 2004, **16**:295-303.
8. Yamashita M, Ukai-Tadenuma M, Kimura M, Omori M, Inami M, Taniguchi M, Nakayama T: **Identification of a conserved GATA3 response element upstream proximal from the interleukin-13 gene locus**. *J Biol Chem* 2002, **277**:42399-42408.
9. Avni O, Lee D, Macian F, Szabo SJ, Glimcher LH, Rao A: **T(H) cell differentiation is accompanied by dynamic changes in histone acetylation of cytokine genes**. *Nat Immunol* 2002, **3**:643-651.
10. Fields PE, Kim ST, Flavell RA: **Cutting edge: changes in histone acetylation at the IL-4 and IFN-gamma loci accompany Th1/Th2 differentiation**. *J Immunol* 2002, **169**:647-650.
11. Baguet A, Bix M: **Chromatin landscape dynamics of the Il4-Il13 locus during T helper 1 and 2 development**. *Proc Natl Acad Sci U S A* 2004, **101**:11410-11415.
12. Yamashita M, Ukai-Tadenuma M, Miyamoto T, Sugaya K, Hosokawa H, Hasegawa A, Kimura M, Taniguchi M, DeGregori J, Nakayama T: **Essential role of GATA3 for the maintenance of type 2 helper T (Th2) cytokine production and chromatin remodeling at the Th2 cytokine gene loci**. *J Biol Chem* 2004, **279**:26983-26990.
13. Zhu J, Min B, Hu-Li J, Watson CJ, Grinberg A, Wang Q, Killeen N, Urban JF Jr, Guo L, Paul WE: **Conditional deletion**

of Gata3 shows its essential function in T(H)1-T(H)2 responses. *Nat Immunol* 2004, **5**:1157-1165.

14. Pai SY, Truitt ML, Ho IC: **GATA-3 deficiency abrogates the development and maintenance of T helper type 2 cells.** *Proc Natl Acad Sci U S A* 2004, **101**:1993-1998.

15. Maurice D, Hooper J, Lang G, Weston K: **c-Myb regulates lineage choice in developing thymocytes via its target gene Gata3.** *EMBO J* 2007, **26**:3629-3640.

16. Wei X, Kee BL: **Growth factor independent 1B (Gfi1b) is an E2A target gene that modulates Gata3 in T-cell lymphomas.** *Blood* 2007, **109**:4406-4414.

17. Dontje W, Schotte R, Cupedo T, Nagasawa M, Scheeren F, Gimeno R, Spits H, Blom B: **Delta-like1-induced Notch1 signaling regulates the human plasmacytoid dendritic cell versus T-cell lineage decision through control of GATA-3 and Spi-B.** *Blood* 2006, **107**:2446-2452.

18. •• Fang TC, Yashiro-Ohtani Y, Del Bianco C, Knoblock DM, Blacklow SC, Pear WS: **Notch directly regulates Gata3 expression during T helper 2 cell differentiation.** *Immunity* 2007, **27**:100-110.
Notch signaling plays multiple roles in Th1/Th2 cell differentiation. This study addressed how Notch mediates Th2 cell differentiation. Notch is shown to regulate GATA3 expression to generate optimal Th2 cell responses.

19. •• Amsen D, Antov A, Jankovic D, Sher A, Radtke F, Souabni A, Busslinger M, McCright B, Gridley T, Flavell RA: **Direct regulation of Gata3 expression determines the T helper differentiation potential of Notch.** *Immunity* 2007, **27**:89-99.
Notch signaling plays multiple roles in Th1/Th2 cell differentiation. This study also addressed how Notch mediates Th2 cell differentiation. By using T-cell-specific ablation of the Notch effector RBP-J or the Notch1 and 2 receptors, these authors show Notch was required for the parasite-induced Th2 cell responses. The regulation of the expression of the GATA3 gene was also demonstrated.

20. Minter LM, Turley DM, Das P, Shin HM, Joshi I, Lawlor RG, Cho OH, Palaga T, Gottipati S, Telfer JC *et al.*: **Inhibitors of gamma-secretase block *in vivo* and *in vitro* T helper type 1 polarization by preventing Notch upregulation of Tbx21.** *Nat Immunol* 2005, **6**:680-688.

21. Maekawa Y, Tsukumo S, Chiba S, Hirai H, Hayashi Y, Okada H, Kishihara K, Yasutomo K: **Delta1-Notch3 interactions bias the functional differentiation of activated CD4+ T cells.** *Immunity* 2003, **19**:549-559.

22. Amsen D, Blander JM, Lee GR, Tanigaki K, Honjo T, Flavell RA: **Instruction of distinct CD4 T helper cell fates by different notch ligands on antigen-presenting cells.** *Cell* 2004, **117**:515-526.

23. Das J, Chen CH, Yang L, Cohn L, Ray P, Ray A: **A critical role for NF-kappa B in GATA3 expression and TH2 differentiation in allergic airway inflammation.** *Nat Immunol* 2001, **2**:45-50.

24. Shin HM, Minter LM, Cho OH, Gottipati S, Fauq AH, Golde TE, Sonenshein GE, Osborne BA: **Notch1 augments NF-kappaB activity by facilitating its nuclear retention.** *EMBO J* 2006, **25**:129-138.

25. Vacca A, Felli MP, Palermo R, Di Mario G, Calce A, Di Giovine M, Frati L, Gulino A, Screpanti I: **Notch3 and pre-TCR interaction unveils distinct NF-kappaB pathways in T-cell development and leukemia.** *EMBO J* 2006, **25**:1000-1008.

26. Kimura MY, Hosokawa H, Yamashita M, Hasegawa A, Iwamura C, Watarai H, Taniguchi M, Takagi T, Ishii S, Nakayama T: **Regulation of T helper type 2 cell differentiation by murine Schnurri-2.** *J Exp Med* 2005, **201**:397-408.

27. Stevens L, Htut TM, White D, Li X, Hanidu A, Stearns C, Labadia ME, Li J, Brown M, Yang J: **Involvement of GATA3 in protein kinase C theta-induced Th2 cytokine expression.** *Eur J Immunol* 2006, **36**:3305-3314.

28. Felli MP, Vacca A, Calce A, Bellavia D, Campese AF, Grillo R, Di Giovine M, Checquolo S, Talora C, Palermo R *et al.*: **PKC theta mediates pre-TCR signaling and contributes to Notch3-induced T-cell leukemia.** *Oncogene* 2005, **24**:992-1000.

29. Yamashita M, Shinnakasu R, Asou H, Kimura M, Hasegawa A, Hashimoto K, Hatano N, Ogata M, Nakayama T: **Ras-ERK MAPK cascade regulates GATA3 stability and Th2 differentiation through ubiquitin–proteasome pathway.** *J Biol Chem* 2005, **280**:29409-29419.

30. Fields PE, Lee GR, Kim ST, Bartsevich VV, Flavell RA: **Th2-specific chromatin remodeling and enhancer activity in the Th2 cytokine locus control region.** *Immunity* 2004, **21**:865-876.

31. Lee DU, Rao A: **Molecular analysis of a locus control region in the T helper 2 cytokine gene cluster: a target for STAT6 but not GATA3.** *Proc Natl Acad Sci U S A* 2004, **101**:16010-16015.

32. Spilianakis CG, Flavell RA: **Long-range intrachromosomal interactions in the T helper type 2 cytokine locus.** *Nat Immunol* 2004, **5**:1017-1027.

33. Lee GR, Spilianakis CG, Flavell RA: **Hypersensitive site 7 of the TH2 locus control region is essential for expressing TH2 cytokine genes and for long-range intrachromosomal interactions.** *Nat Immunol* 2005, **6**:42-48.

34. •• Cai S, Lee CC, Kohwi-Shigematsu T: **SATB1 packages densely looped, transcriptionally active chromatin for coordinated expression of cytokine genes.** *Nat Genet* 2006, **38**:1278-1288.
SATB1 (special AT-rich sequence binding protein 1) is known to organize the cell-type-specific nuclear architecture by anchoring specialized DNA sequences, and recruit chromatin remodeling factors to control the transcription of the various genes. Chromatin loop analyses in Th2 cells revealed that SATB1 is important for the formation of high-order chromatin structure around the Th2 cytokine gene loci.

35. Ansel KM, Greenwald RJ, Agarwal S, Bassing CH, Monticelli S, Interlandi J, Djuretic IM, Lee DU, Sharpe AH, Alt FW *et al.*: **Deletion of a conserved Il4 silencer impairs T helper type 1-mediated immunity.** *Nat Immunol* 2004, **5**:1251-1259.

36. • Djuretic IM, Levanon D, Negreanu V, Groner Y, Rao A, Ansel KM: **Transcription factors T-bet and Runx3 cooperate to activate Ifng and silence Il4 in T helper type 1 cells.** *Nat Immunol* 2007, **8**:145-153.
Runx3 is shown to be a potential regulator of HSIV (IL-4 silencer)-mediated IL-4 gene silencing in Th1 cells. Th1 cells that lack the HSVI are less sensitive to the repression of IL-4 production by T-bet or Runx3.

37. • Naoe Y, Setoguchi R, Akiyama K, Muroi S, Kuroda M, Hatam F, Littman DR, Taniuchi I: **Repression of interleukin-4 in T helper type 1 cells by Runx/Cbf beta binding to the Il4 silencer.** *J Exp Med* 2007, **204**:1749-1755.
Runx3 is shown to be a potential regulator of HSIV (IL-4 silencer)-mediated IL-4 gene silencing in Th1 cells. The enforced expression of GATA3 in Th1 cells induced the dissociation of the Runx complex from the IL-4 silencer.

38. Li B, Carey M, Workman JL: **The role of chromatin during transcription.** *Cell* 2007, **128**:707-719.

39. •• Yamashita M, Hirahara K, Shinnakasu R, Hosokawa H, Norikane S, Kimura MY, Hasegawa A, Nakayama T: **Crucial role of MLL for the maintenance of memory T helper type 2 cell responses.** *Immunity* 2006, **24**:611-622.
The authors report that MLL, a *Trithorax* gene product is required for the maintenance of memory Th2 cell function. MLL possesses an intrinsic histone methyltransferase (H3-K4) activity. This is the first example of the identification of a molecule that controls the function of memory Th cells.

40. Bernstein BE, Kamal M, Lindblad-Toh K, Bekiranov S, Bailey DK, Huebert DJ, McMahon S, Karlsson EK, Kulbokas EJ 3rd, Gingeras TR *et al.*: **Genomic maps and comparative analysis of histone modifications in human and mouse.** *Cell* 2005, **120**:169-181.

41. Yokoyama A, Wang Z, Wysocka J, Sanyal M, Aufiero DJ, Kitabayashi I, Herr W, Cleary ML: **Leukemia proto-oncoprotein MLL forms a SET1-like histone methyltransferase complex with menin to regulate Hox gene expression.** *Mol Cell Biol* 2004, **24**:5639-5649.

42. • Kimura MY, Iwamura C, Suzuki A, Miki T, Hasegawa A, Sugaya K, Yamashita M, Ishii S, Nakayama T: **Schnurri-2 controls memory Th1 and Th2 cell numbers *in vivo*.** *J Immunol* 2007, **178**:4926-4936.
The generation of memory Th1 and Th2 cells is regulated by Schnurri-2, a C2H2 type zinc finger transcription factor. Deactivation of NF-κB at the

contraction phase is demonstrated to be required for generating a sufficient number of memory Th1 and Th2 cells. A crucial transcription factor that regulates the number of memory Th1/Th2 cells is identified.

43. Luckey CJ, Bhattacharya D, Goldrath AW, Weissman IL, Benoist C, Mathis D: **Memory T and memory B cells share a transcriptional program of self-renewal with long-term hematopoietic stem cells.** *Proc Natl Acad Sci U S A* 2006, **103**:3304-3309.

44. Yamashita M, Kuwahara M, Suzuki A, Hirahara K, Shinnakasu R, Hosokawa H, Hasegawa A, Motohashi S, Iwama A, Nakayama T: **Bmi1 regulates memory CD4 T cell survival via repression of the Noxa gene.** *J Exp Med* 2008, **205**:1087-1097.

Journal of Urban Health: Bulletin of the New York Academy of Medicine
doi:10.1007/s11524-008-9264-0

Preparedness for the Spread of Influenza: Prohibition of Traffic, School Closure, and Vaccination of Children in the Commuter Towns of Tokyo

Hidenori Yasuda, Nobuaki Yoshizawa, Mikio Kimura, Mika Shigematsu, Masaaki Matsumoto, Shoji Kawachi, Masamichi Oshima, Kenji Yamamoto, and Kazuo Suzuki

ABSTRACT *In Greater Tokyo, many people commute by train between the suburbs and downtown Tokyo for 1 to 2 h per day. The spread of influenza in the suburbs of Tokyo should be studied, including the role of commuters and the effect of government policies on the spread of disease. We analyzed the simulated spread of influenza in commuter towns along a suburban railroad, using the individual-based Monte Carlo method, and validated this analysis using surveillance data of the infection in the Tokyo suburbs. This simulation reflects the mechanism of the real spread of influenza in commuter towns. Three measures against the spread of influenza were analyzed: prohibition of traffic, school closure, and vaccination of school children. Prohibition of traffic was not effective after the introduction of influenza into the commuter towns, but, if implemented early, it was somewhat effective in delaying the epidemic. School closure delayed the epidemic and reduced the peak of the disease, but it was not as effective in decreasing the number of infected people. Vaccination of school children decreased the numbers not only of infected children but also of infected adults in the regional communities.*

KEYWORDS *Influenza, Computer simulation, Commuters, Prohibition of traffic, School closure, Vaccination*

Abbreviations: PT – prohibition of traffic; SC – school closure; VSC – vaccination of school children; PHC – Public Health Center; NIID – National Institute of Infectious Diseases

Yasuda is with the Department of Mathematics, Josai University, Saitama, Sakado, Japan; Yoshizawa and Matsumoto are with the Mitsubishi Research Institute, Inc., Tokyo, Chiyoda-ku, Japan; Kimura is with the Japan Anti-Tuberculosis Association, Higashimurayama, Japan; Shigematsu, Oshima, and Suzuki are with the National Institute of Infectious Diseases, Tokyo, Shinjuku-ku, Japan; Kawachi and Yamamoto are with the International Medical Center in Japan, Tokyo, Shinjuku-ku, Japan; Suzuki is with the Inflammation Program, Department of Immunology, Chiba University Graduate School of Medicine, Chiba, Japan; Suzuki is with the Department of Immunology, National Institute of Infectious Diseases, Shinjuku-ku, Tokyo, Japan.

Correspondence: Kazuo Suzuki, PhD, Inflammation Program, Department of Immunology, Chiba University Graduate School of Medicine, Chiba, 260-8670, Japan. (E-mail: ksuzuki@nih.go.jp, ksuzuki@faculty.chiba-u.jp)

INTRODUCTION

If a pandemic influenza were to spread across the capital city of Tokyo, extensive damage to health, life, and the economy could be expected. To reduce the risk of such damage, we must understand the mechanisms of the spread of seasonal influenza in the commuter towns of Tokyo, and we must be prepared for this event. This study is a simulation based on national sentinel surveillance data of seasonal influenza. Simulation is a useful tool for helping administrators plan their actions against influenza. Past experience is of vital importance; however, environmental conditions change with time, and little information is currently available for emerging influenza. It is also very difficult to perform social experiments in the real world.

To design preventative measures against influenza, prohibition of traffic (PT), school closure (SC), and vaccination of school children (VSC) were simulated. Many people who work in Tokyo during the day commute by railroad 1 or 2 h per day. Because the commuters comprise $\approx$10% of the population of suburban towns, commuters would play an important role in the spread of influenza in the suburbs of Tokyo. PT is a possible candidate for the prevention of disease, but this has not thus far been implemented. Moreover, SC is often adopted when school children contract influenza, but the effect of SC is still undetermined. In Japan, children were mass-vaccinated by law from 1962 to 1987. However, in 1987, this law was relaxed, and it was repealed in 1994 because an efficient flu vaccine was not considered important at that time. A recent study[1] shows the possibility that VSC prevents influenza from spreading in the community; this possibility should be explored by the simulation of new situations and by undertaking new measures.

Many studies of the simulated spread of influenza have analyzed a local seasonal epidemic, without traffic to other regions.[2–7] However, considering the threat of avian flu, whether influenza is contained in a local region or transmitted to other regions will make a great difference. Longini et al.[8,9] investigated the possibility of containing avian flu within a region of Southeast Asia and within the United State. Ferguson et al.[10] also investigated the same possibility in Thailand. The transmission of influenza as a multicity problem in the United States was studied by simulation[11], and a theoretical analysis was performed.[12] These study protocols are useful for simulating the spread of influenza in the commuter towns of Tokyo, where the distinctive feature is the important role played by commuters. Virtual communities along the suburban railroad are constructed for commuter-focused simulation, based on Japanese social statistics: Japanese census data, the statistics of local governments of greater Tokyo, and a survey of Tokyo metropolitan region transportation.

In our simulation, recent real infection data of seasonal influenza during three seasons from 2002 to 2006 was used for understanding the mechanism of the spread of influenza in the suburbs of Tokyo. Influenza infection in Japan is reported from 5,000 sentinel points (designated monitoring points) and data accumulated at regional Public Health Centers (PHC, healthcare centers), then reported to the National Institute of Infectious Disease (NIID). NIID officially announces a seasonal influenza epidemic when the number of patients reported from a sentinel point exceeds 30 per week. For the winter of 2002/2003 and 2003/2004, the maximum number of patients reported per week from a sentinel point was more than 20 but less than 30 in Tokyo. For the winter of 2005/2006, it was greater than 40.

In the present study, we simulated the spread of influenza across the capital city of Tokyo to collect information for measures to mitigate the damage of a pandemic influenza using the individual-based Monte Carlo method. We chose the major suburban

railroad Chuo Line in western Tokyo as a virtual railroad (Figure 1). We analyzed Japanese national surveillance data and used these data to verify our simulations of the mechanism of the real spread of influenza. In addition, we estimated three measures against influenza: (1) PT, (2) SC, and (3) VSC, using the probabilities of the transmission of seasonal influenza in the literature[2–7] because that of emerging influenza is unknown. We also analyzed the effects of low-dose vaccination administered to children in our simulation. Because a short supply of the vaccine due to large-scale distribution during pandemic influenza may result in low-dose inoculation, lower efficiency of vaccination is expected. Finally, the combined effect of these measures was analyzed by simulation.

METHODS

Simulation

We performed Monte Carlo simulation using an individual-based model. We constructed a regional simulated community called the virtual Chuo Line. First, we generated individual people. The number of people in each town was proportional to the number of commuters; the total number of people generated was 8,800. Two thousand people were generated in Hachoji City, 2,600 in Tachikawa City, 2,800 in the Kichijoji area of Musashino City, and the rest were in Shinjuku and Tokyo. Our model was scaled down, but preliminary estimates showed 8,800 people were sufficient for Monte Carlo simulation. These people were connected to many different types of families: singles, couples, fathers, mothers, and children. The ratio of types of families was determined by Japanese census data.

We also constructed "compartments," consisting of 4,040 homes, 60 schools, 658 companies, and 117 stores, using local government statistics. For commuters, the data of the fourth Person Trip Survey of Tokyo Metropolitan Region Transportation was used. In this model, 12% of the people in the suburbs are commuters. We operated trains that moved between stations according to a railroad timetable.

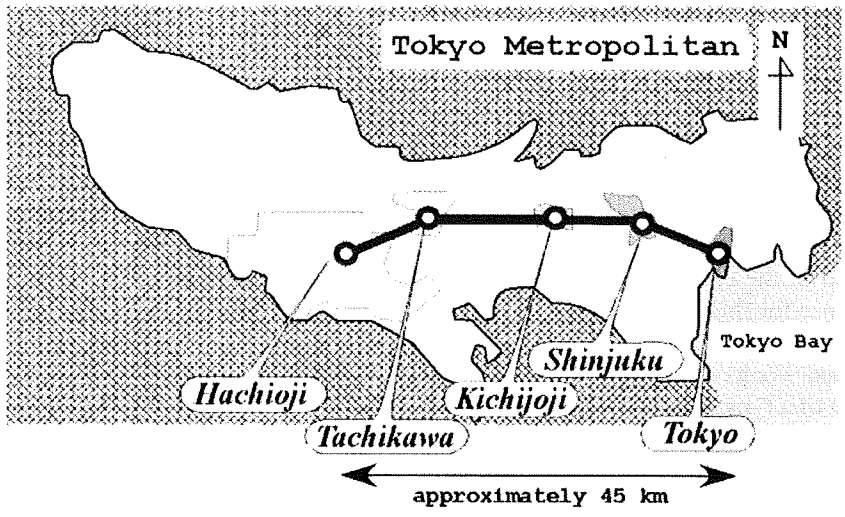

FIGURE 1. Location of stations along the virtual Chuo Line in Tokyo. The Hachioji, Tachikawa, and Kichijoji Stations are located west of Tokyo. The Shinjuku and Tokyo Stations are in the Tokyo central area. The *outlines* are the prefecture boundaries of Greater Tokyo.

Homes, schools, companies, and stores are fixed compartments, and trains are moving compartments. As timetables, we gave people event histories, consisting of movement from one compartment to another. Event histories were constructed using statistical data of the daily life of ≈30,000 Japanese people.[13] In these compartments, people contacted each other stochastically and were occasionally infected. The probabilities of infection we used were 0.005/h for homes, 0.0016 for schools, 0.0125 for trains, and 0.00001 for companies and stores. The width of a time step in our simulation was 1 h, and we used probabilities per hour. The probabilities of infection have been studied in the literature,[2–7] where probabilities are values per day. For homes, schools, companies, and stores, converting each unit with the reasonable assumption that employees are at work from 9:00 A.M. to 5:00 P.M., our values are in the range of those in the literature. For the probability of trains, we assumed they were densely packed. Medical conditions were specified by a scenario of infection in which the latent time was 2 days, and the period of infection was 5 days. In the simulation, all infected people eventually recovered.

Surveillance Data of Infectious Disease

The Ministry of Health, Labour and Welfare reports surveillance data of infectious disease through registration with the NIID, to which every PHC reports the number of newly infected patients every week. The data of the PHCs come from fixed medical agencies in Japan, consisting of 3,000 pediatricians and 2,000 internists. There are three PHCs in the suburbs along the Chuo Line. The Hachioji PHC is near Hachioji Station; the Tama-Tachikawa PHC, near Tachikawa Station; and the Sugunami PHC, near Kichijoji Station. We analyzed the data from the end of 2002 to the beginning of 2006.

RESULTS

Simulation of the Spread of Influenza in the Suburbs along the Chuo Line in Tokyo

We performed preliminary simulations primarily to specify where the first persons were infected. We tried four situations, in which the first persons infected were in Hachioji, Tachikawa, Kichijoji, or Tokyo. For the situation where the first person infected was in Tokyo, commuters were the first to be infected. In the other three situations, the spread of the epidemic in the town where the first person infected was preceded by infection in the other towns along Chuo Line. This is because the spread of infection among school children in the first town was faster than transmission to the other towns by commuters. When the first person seeded in Tokyo, the causes of the spread of the epidemic almost coalesced in every year examined. Below, we present evidence for this using real data. Our simulation focused on the last situation.

There were similarities among the results of cases where commuters were the first infected. We have discussed the case where ten commuters were the first infected. The graph of a typical result (Figure 2A) shows the number of infected living in the areas of Hachioji, Tachikawa, and Kichijoji Stations. The number of infected living in Hachioji was 572, 914 in Tachikawa, and 1,108 in Kichijoji, respectively. The total number of infected along the Chuo Line, including the initial 10 infected commuters, was 2,915, which is 33% of the population along the Chuo Line. At the beginning of the spread of influenza, there was a period when the number of infected was small, then increased exponentially. The peaks of the number of infected in three towns coalesced ≈6 weeks after the beginning of the spread of influenza.

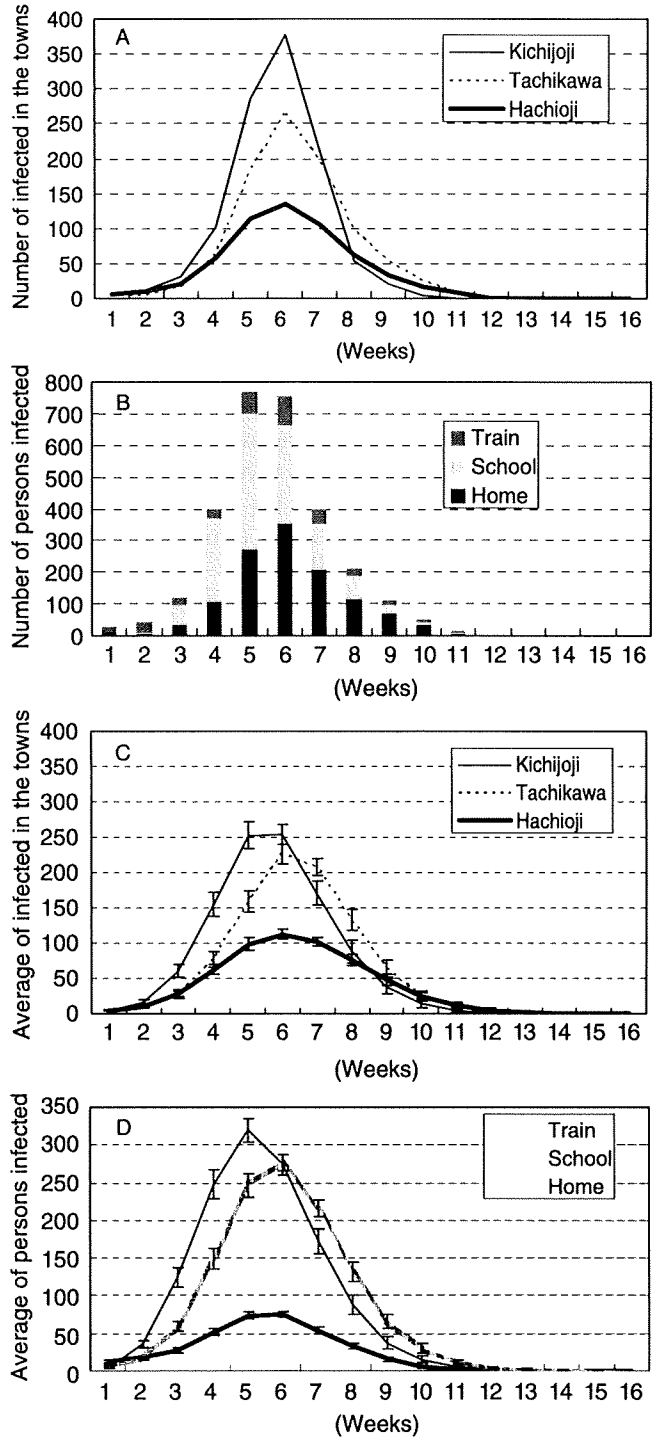

FIGURE 2. Influenza spread along the virtual Chuo Line. **A** The number of infected who live in each commuter town in a typical case. **B** The number of persons newly infected divided by location of a typical case. **C** The average of 100 cases of infected who live in each commuter town. **D** The average of 100 cases of persons newly infected divided by place. *Bars* indicate 95% confidence interval.

Figure 2B shows the number of persons newly infected, including where they became infected. In the beginning, a small number of persons were consistently infected in trains. Infections in schools then increased, followed by homes; there were few occurrences in companies and stores. Figure 2C and D show the average of 100 cases in the Monte Carlo simulation. Because the peaks are out of synchronization, the peak of the average appears lower than that of the typical case.

Real Data of the Spread of Influenza in the Suburbs along the Chuo Line

With the permission of the NIID, we analyzed the number of notifications from the Hachioji, Tama-Tachikawa, and Suginami PHCs from the end of 2002 to early 2006. Type A influenza was detected in the winter of 2002–2003, 2003–2004, and 2005–2006, but in 2004–2005, type A was detected in early winter and type B in late winter. Figure 3 shows the number of notifications from these three PHCs in the winter of 2002–2003, 2003–2004, and 2005–2006. As shown in Figure 3, the data during the period from the 45th week of a given year to the 15th week of next year are shown. The number of patients infected with influenza remained small at the beginning of the season and then increased exponentially. Peaks of infection almost coalesced in each town. These profiles are similar to the profiles of our simulation. In some cases, peaks appeared in early winter and disappeared due to the New Year holidays.

Simulation of Measures Against the Spread Of Influenza

We proposed three measures against the spread of epidemic influenza: (1) PT, (2) SC, and (3) VSC. For each measure, the profiles of the number of persons infected in simulated cases were similar. We utilized the same commuters with the case in Figure 2 as the first persons infected as the basic scenario for this analysis. The scenarios of the simulation in the case in Figure 2 were modified for PT, SC, and VSC. We show the results of a typical case and the average results of 100 cases for each scenario.

For PT, we assumed a 2-week prohibition of the virtual Chuo Line, starting with the fourth week after the beginning of the epidemic. Figure 4A shows the number of persons infected in a typical case divided into specific locations during PT. The total number of persons newly infected is 2,872, without the initial 10. Figure 4D shows the average number of persons newly infected; the total number is 2,837.

For SC, schools were closed for 2 weeks, starting with the fourth week after the beginning of the epidemic. Figure 4B shows the number of persons infected in a typical case. The total number of persons newly infected was 2,813. Figure 4E shows the average number of persons newly infected; the total number is 2,696.

For VSC, we assume children were vaccinated before the influenza season. In this study, instead of conventional vaccination that could not be specified before simulation, we used the fraction of vaccinated children who become immune as a parameter: the percentage of unsusceptible children, x, means x number of 100 vaccinated children would become immune. Figure 4C, a typical case, shows the number of persons infected if 30% of children would become unsusceptible. The total number of persons newly infected is 1,786; Figure 4F shows the average. The average number of persons newly infected in cases of 5–30% of unsusceptible children is shown in Table 1. For 30%, the total number is 1,761. Using the results of the simulation, we define the conventional efficiency of the vaccination of the community in Table 1 as 1 minus the ratio of the number of infected in the community in the case of VSC to the number of infected in the community in the case of unvaccinated children. When the

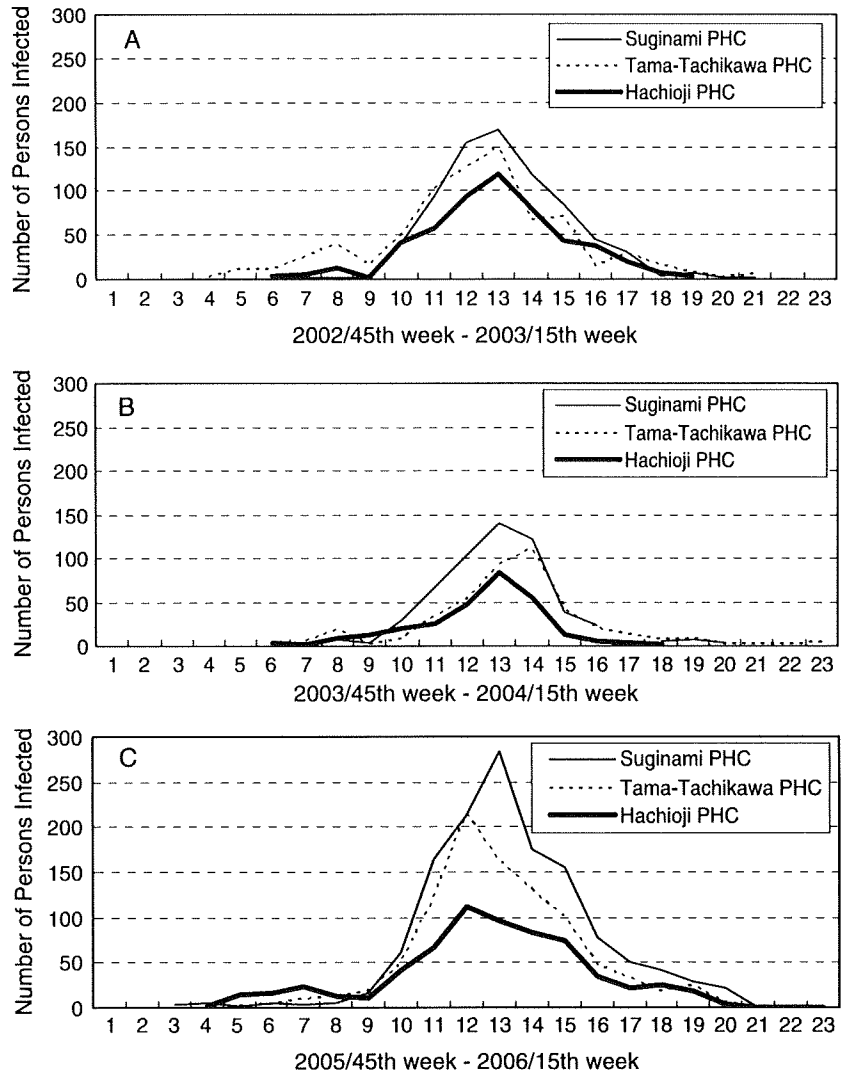

FIGURE 3. Data of notification of influenza from the PHC along the Chuo Line. Data of the Suginami, Tama-Tachikawa, and Hachioji PHCs during the period from the 45th week of a given year to the 15th week of the next year. **A** Data from the end of 2002 to 2003, **B** the end of 2003 to 2004, and **C** the end of 2005 to 2006. Suginami PHC is near Kichijoji Station; Tama-Tachikawa PHC, near Tachikawa Station; and Hachioji PHC, near Hachioji Station.

number of persons infected in the schools decreased, the efficiency of the vaccination of the community increased.

The spread of an epidemic would be affected by PT or SC in the early stages of an epidemic. The numbers of infected if PT started (1) 3 days, (2) 1 week, (3) 2 weeks, (4) 3 weeks, or (5) 4 weeks after the beginning of the epidemic are compared in Figure 5A. The average of the total number of newly infected was 2,909 for (1), 2,943 for (2), 2,915 for (3), 2,874 for (4), and 2,837 for (5). The variation of the total number of persons infected is less than 4% of the number of infected in the case without any implemented preventative measures. For compar-

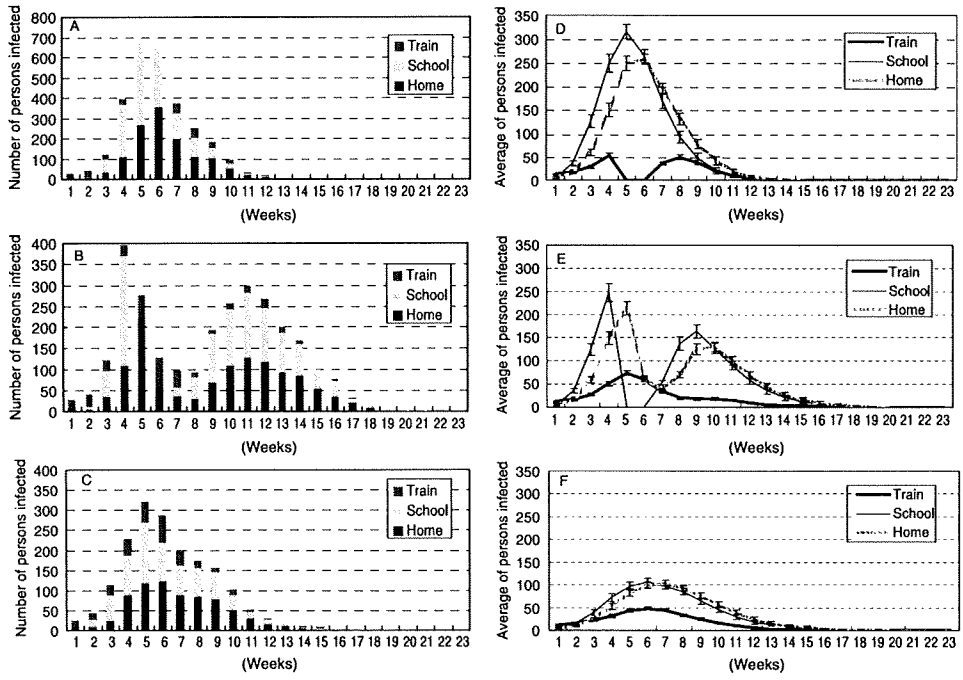

FIGURE 4. Number of persons infected in different anti-influenza scenarios. **A** The number of persons infected in a typical case when traffic was prohibited 4 weeks after the beginning of the epidemic for 2 weeks, divided into locations. **B** SC 4 weeks after the beginning of epidemic for 2 weeks. **C** Vaccination, where the percent of unsusceptible children in C is 30%. **D** The average of 100 cases of persons infected when traffic was prohibited 4 weeks after the beginning of the epidemic for 2 weeks. **E** The average of 100 cases of SC 4 weeks after the beginning of the epidemic for 2 weeks. **F** The average of 100 cases of vaccination, where the percent of unsusceptible children is 30%. *Bars* indicate 95% confidence interval.

TABLE 1. Number of persons infected when vaccination is implemented

	Unsusceptible children				
Parameter	0%	5%	10%	20%	30%
Infected in trains	376 (371–380)	371 (366–375)	358 (353–362)	344 (339–348)	317 (305–328)
Infected in schools	1,332 (1,327–1,336)	1,234 (1,229–1,238)	1,131 (1,126–1,135)	936 (931–940)	709 (683–734)
Infected in homes	1,227 (1,219–1,234)	1,143 (1,135–1,150)	1,062 (1,054–1,069)	913 (905–920)	722 (696–747)
Newly infected children	1,615 (1,610–1,619)	1,495 (1,490–1,499)	1,371 (1,365–1,376)	1,147 (1,141–1,152)	878 (846–909)
Newly infected adults	2,951 (2,939–2,962)	2,765 (2,753–2,776)	2,567 (2,554–2,579)	2,207 (2,195–2,218)	1,761 (1,698–1,823)
Efficiency of vaccination to community		6.3%	13.0%	25.2%	40.3%

(-) 95% confidence interval.